



TITLE:

# Production and nonclinical evaluation of an autologous iPSC-derived platelet product for the iPLAT1 clinical trial

AUTHOR(S):

Sugimoto, Naoshi; Nakamura, Sou; Shimizu, Shin; Shigemasa, Akiko; Kanda, Junya; Matsuyama, Nobuki; Tanaka, Mitsunobu; ... Tani, Yoshihiko; Takaori-Kondo, Akifumi; Eto, Koji

---

CITATION:

Sugimoto, Naoshi ...[et al]. Production and nonclinical evaluation of an autologous iPSC-derived platelet product for the iPLAT1 clinical trial. *Blood Advances* 2022, 6(23): 6056-6069

ISSUE DATE:

2022-12-13

URL:

<http://hdl.handle.net/2433/277805>

RIGHT:

© 2022 by The American Society of Hematology.; Licensed under Creative Commons Attribution-NonCommercial-NoDerivatives 4.0 International (CC BY-NC-ND 4.0), permitting only noncommercial, nonderivative use with attribution. All other rights reserved.

# Production and nonclinical evaluation of an autologous iPSC-derived platelet product for the iPLAT1 clinical trial

Naoshi Sugimoto,<sup>1,\*</sup> Sou Nakamura,<sup>1,\*</sup> Shin Shimizu,<sup>1</sup> Akiko Shigemasa,<sup>1</sup> Junya Kanda,<sup>2</sup> Nobuki Matsuyama,<sup>3</sup> Mitsunobu Tanaka,<sup>3</sup> Tomoya Hayashi,<sup>3</sup> Akihiro Fuchizaki,<sup>3</sup> Masayuki Nogawa,<sup>4</sup> Naohide Watanabe,<sup>5</sup> Shinichiro Okamoto,<sup>5</sup> Makoto Handa,<sup>6</sup> Akira Sawaguchi,<sup>7</sup> Dai Momose,<sup>8</sup> Ki-Ryang Koh,<sup>8</sup> Yoshihiko Tani,<sup>3</sup> Akifumi Takaori-Kondo,<sup>2</sup> and Koji Eto<sup>1</sup>

<sup>1</sup>Department of Clinical Application, Center for iPSC Cell Research and Application (CiRA), Kyoto University, Kyoto, Japan; <sup>2</sup>Department of Hematology, Kyoto University Hospital, Kyoto, Japan; <sup>3</sup>Japanese Red Cross Kinki Block Blood Center, Osaka, Japan; <sup>4</sup>Central Blood Institute, Blood Service Headquarters, Japanese Red Cross Society, Tokyo, Japan; <sup>5</sup>Division of Hematology, Keio University School of Medicine, Tokyo, Japan; <sup>6</sup>Center for Transfusion Medicine & Cell Therapy, Keio University School of Medicine, Tokyo, Japan; <sup>7</sup>Department of Anatomy, Faculty of Medicine, University of Miyazaki, Miyazaki, Japan; and <sup>8</sup>Department of Hematology, Osaka General Hospital of West Japan Railway Company, Osaka, Japan

## Key Points

- GMP-based iPSC-platelet production using imMKCL master cells from an aplastic anemia patient with alloimmune transfusion refractoriness.
- Extensive nonclinical evaluation confirmed the safety, quality, and efficacy of the patient iPSC-platelet product.

Donor-derived platelets are used to treat or prevent hemorrhage in patients with thrombocytopenia. However, ~5% or more of these patients are complicated with alloimmune platelet transfusion refractoriness (allo-PTR) due to alloantibodies against HLA-I or human platelet antigens (HPA). In these cases, platelets from compatible donors are necessary, but it is difficult to find such donors for patients with rare HLA-I or HPA. To produce platelet products for patients with aplastic anemia with allo-PTR due to rare HPA-1 mismatch in Japan, we developed an ex vivo good manufacturing process (GMP)-based production system for an induced pluripotent stem cell-derived platelet product (iPSC-PLTs). Immortalized megakaryocyte progenitor cell lines (imMKCLs) were established from patient iPSCs, and a competent imMKCL clone was selected for the master cell bank (MCB) and confirmed for safety, including negativity of pathogens. From this MCB, iPSC-PLTs were produced using turbulent flow bioreactors and new drugs. In extensive nonclinical studies, iPSC-PLTs were confirmed for quality, safety, and efficacy, including hemostasis in a rabbit model. This report presents a complete system for the GMP-based production of iPSC-PLTs and the required nonclinical studies and thus supports the iPLAT1 study, the first-in-human clinical trial of iPSC-PLTs in a patient with allo-PTR and no compatible donor using the autologous product. It also serves as a comprehensive reference for the development of widely applicable allogeneic iPSC-PLTs and other cell products that use iPSC-derived progenitor cells as MCB.

## Introduction

The transfusion of  $2\text{-}3 \times 10^{11}$  platelet products from blood donors is commonly done to prevent or treat bleeding complications in patients with thrombocytopenia.<sup>1,2</sup> However, alloimmune platelet transfusion refractoriness (allo-PTR) is present in approximately 5% to 15% of the patients who undergo platelet transfusion.<sup>3</sup> Gestation or previous platelet transfusion leads to sensitization against platelet alloantigens such as HLA-I and human platelet antigen (HPA).<sup>3</sup> As a clinical measure for

Submitted 8 July 2022; accepted 16 August 2022; prepublished online on *Blood Advances* First Edition 23 September 2022. <https://doi.org/10.1182/bloodadvances.2022008512>.

\*These authors contributed equally.

Data are available on request from the corresponding author, Koji Eto ([kojiето@cira.kyoto-u.ac.jp](mailto:kojiето@cira.kyoto-u.ac.jp)).

The full-text version of this article contains a data supplement.

© 2022 by The American Society of Hematology. Licensed under [Creative Commons Attribution-NonCommercial-NoDerivatives 4.0 International \(CC BY-NC-ND 4.0\)](https://creativecommons.org/licenses/by-nc-nd/4.0/), permitting only noncommercial, nonderivative use with attribution. All other rights reserved.

transfusion in allo-PTR, blood products from compatible donors are transfused,<sup>3</sup> but these donors are difficult to recruit for very rare platelet types.

Induced pluripotent stem cells (iPSCs) can be a source for producing essentially perfectly compatible autologous differentiated cells.<sup>4-8</sup> However, extensively expanding iPSCs and then differentiating them into mature megakaryocytes to produce 10<sup>11</sup>-scale platelets is a long and inefficient process requiring huge labor and cost.<sup>9,10</sup> To overcome these limitations, we established immortalized megakaryocyte progenitor cell lines (imMKCLs) from iPSCs.<sup>11</sup> In the presence of doxycycline in the medium, imMKCLs expand by the expression of 3 transgenes, *c-MYC*, *BMI1*, and *BCL-XL*. Upon depletion of doxycycline, imMKCLs cease to express these transgenes, causing the cells to mature and generate an iPSC-derived platelet product, iPSC-PLTs. We then developed a thrombopoietin receptor agonist, TA-316,<sup>12</sup> and an inhibitor of a disintegrin and metalloproteinase domain-containing protein 17 (ADAM17), KP-457, which prevents the shedding of GPIIb from platelets.<sup>13</sup> We also discovered that the combination of an arylhydrocarbon receptor antagonist and a Rho-associated kinase inhibitor enables the feeder cell-independent production of iPSC-PLTs.<sup>14</sup> We further developed a turbulent flow-type VerMES bioreactor based on the findings that turbulence markedly enhances thrombopoiesis. Through these developments, we acquired the capacity to produce the clinical order of 10<sup>11</sup>-scale competent iPSC-PLTs ex vivo in a liquid tank.<sup>14</sup>

Based on this success, we aimed to provide an autologous platelet product for a patient with aplastic anemia with allo-PTR, who did not have a compatible HPA-1b/1b platelet donor in Japan. Here, we report the good manufacturing practice (GMP)-based production and extensive preclinical assessment of autologous iPSC-PLTs using imMKCLs as the master cell bank (MCB). This work has led to a clinical trial, iPLAT1, which was completed in 2021 and the results submitted to *Blood*.

## Methods

### Oversight

The study to establish imMKCLs and produce iPSC-PLTs from the patient was ethically approved by Kyoto University and conducted in accordance with the Declaration of Helsinki. The patient had the rare HPA-1b/1b phenotype in Japan and bore anti-HPA1a antibodies. She had never been transfused with platelets previously, suggesting that gestation was the cause of sensitization. The relative frequency of the HPA-1b allele was 0.4% in Japan. Therefore, the HPA-1b/1b phenotype was calculated to be <0.002% in the Japanese population,<sup>15</sup> and there was no suitable blood donor in the Japanese Red Cross Society (JRC) registry. Written informed consent was obtained from the patient. Experiments involving the use of samples obtained from human and animal studies were reviewed and approved by the institutional review board at Kyoto University and Keio University.

imMKCLs were established at the Center for Cell and Molecular Therapy, Kyoto University Hospital, and shipped to the facility for iPSC Cell Therapy, Kyoto University Center for iPSC Cell Research and Application (CiRA) Foundation, after the Center for Cell and Molecular Therapy facility manager confirmed the quality test reports, manufacturing records, manufacturing management, and

deviation and issued the manufacturing and shipping confirmation. The details of the production methods are provided in the supplemental material.

### Flow cytometry analysis

For megakaryocyte surface markers, cells were stained with the following antibodies: allophycocyanin (APC)-anti-hCD41a (Biolegend, #303710), phycoerythrin (PE)-anti-hCD42b (Biolegend, #303906), and Pacific blue-anti-hCD235ab (Biolegend, #306612).

To quantify platelets, the samples were stained with APC-anti-hCD41a and PE-anti-hCD42b antibodies. After incubating in the dark for 20 minutes at room temperature, HEPES-Tyrode buffer was added, and the platelet count was measured using TruCount beads (BD Biosciences, #340334).

To measure annexin V binding levels, samples were stained with an APC-anti-hCD41a antibody and V450-annexin V (BD Biosciences, #560506). After incubation at room temperature in the dark for 20 minutes, annexin buffer was added to the samples, and the mixtures were analyzed. As a maximum positive control, 100  $\mu$ L of platelet samples were added to 2  $\mu$ L of 1 mM ionomycin before the addition of the antibodies.

To measure PAC-1 binding and P-selectin expression levels, the samples were mixed with or without phorbol-12-myristate-13-acetate (PMA; 0.2  $\mu$ M final) or adenosine tri-phosphate (ADP) + thrombin receptor activator peptide 6 (TRAP6) (100  $\mu$ M and 40  $\mu$ M final, respectively) and then with APC-anti-hCD62P (Biolegend, #304910), PE-anti-hCD41a (Bio Legend, 303706), and fluorescein isothiocyanate (FITC)-PAC-1 (BD Biosciences, #340507) antibodies. After incubation for 30 minutes at room temperature in the dark, the samples were mixed with HEPES-Tyrode buffer and analyzed.

To measure the surface expression of AB antigens, iPSC-PLTs or JRC donor-derived platelets (JRC-PLTs) were stained with mouse antihuman A or B immunoglobulin M (Ortho-Clinical Diagnostics ABO Blood Group Reagents) or isotype control. FITC-goat-anti-mouse immunoglobulin G (BD Biosciences, #554001) was used as the secondary antibody and normal mouse serum (Invitrogen, #10410) was as the blocking reagent. The PerCP-Cy5.5-anti-hCD41a antibody (BD Biosciences, #340931) was added last.

To measure the surface expression of HPAs and HLA class I, iPSC-PLTs or JRC-PLTs were stained with the following antibodies: FITC-anti-hCD42b (clone SZ2, Beckman Coulter, IM06480), FITC-anti-hCD61 (clone: RUU-PL 7F12, BD Biosciences, #348093), FITC-anti-hCD36 (Beckman Coulter, PN IM0766U), FITC-anti-hCD49b (clone J4.57, Beckman Coulter, PN IM1424), FITC-anti- HLA-A/B/C (BD Biosciences, #555552), FITC-anti-hCD61 (clone: SZ21, Beckman Coulter, IM1758), and FITC-mouse isotype control (BD Biosciences, #349041). To gate the platelet population, PE-anti-hCD42b (clone AN51, BD Biosciences, #555473), PE-mouse isotype control (BD Biosciences, #349043), PerCP-mouse isotype control, and PerCP-Cy5.5-anti-hCD41a (BD Biosciences, #340931) were used.

All samples were analyzed with fluorescence-activated cell sorting (FACS) Verse, FACSAria, or FACSCanto II (BD Biosciences).

## Genotyping and MR-MAIPA assay

For genotyping, genome DNA was extracted from cells using a QuickGene DNA whole blood kit (DB-S, Kurabo Biomedical). The extracted DNA was amplified using multiplex polymerase chain reaction (PCR), hybridized to oligonucleotide probes immobilized on microsphere beads, labeled with SAPE using WAKFlow HPA typing reagents (4R408, Wakunaga Pharmaceutical), and analyzed using Luminex XYP.

For the modified rapid monoclonal antibody-specific immobilization of platelet antigens (MR-MAIPA) assay,<sup>16</sup> platelet samples were added to anti-HPA-1a sera or negative control serum and capture antibodies: anti-hCD41 (clone HIP8; Biolegend, #303702), anti-hCD41 (clone P2; Beckman Coulter, PN IM0145), or anti-hCD61 (clone SZ21; Beckman Coulter, IM0540). After lysing the platelets, samples were applied to anti-mouse IgG antibody-coated plates, washed, mixed with peroxidase-goat-anti-human IgG antibody (Jackson ImmunoResearch Laboratories, #109-035-088), and subjected to fluorescence by the addition of a substrate (KPL, #50-76-00). The reaction was then stopped by the addition of 3, 3', 5, 5'-tetramethylbenzidine stop solution (KPL, #50-85-05), and the absorbance was measured at 450 nm (MTP-120, Hitachi, Tokyo, Japan).

## Platelet size and IPF measurements

The size of the platelets was measured using a particle size analyzer (JASCO international, IF-200 nano). Immature platelet fraction (IPF) was measured using an automated hematology analyzer (Sysmex, XN-1000).

## Platelet aggregation assay

Assays were performed using an aggregation analyzer (Kowa PA-200C). The iPSC-PLTs were resuspended in 70% human plasma ( $3 \times 10^8$  platelets per mL) with 3 mM calcium chloride. Sample preparation (270  $\mu$ L) was mixed with 30  $\mu$ L of stimuli solution including, 5, 10, or 20  $\mu$ g/mL collagen or 50  $\mu$ M ADP for 8 minutes at 37°C.

## Electron microscopy

Platelet pellets were fixed using a mixture of 0.5% glutaraldehyde and 2% paraformaldehyde in 0.1 M phosphate buffer (pH 7.4) for 10 minutes at room temperature. After washing with phosphate buffer, the samples were postfixed with 1% osmium tetroxide in phosphate buffer for 60 minutes on ice. After dehydration, the samples were infiltrated with and embedded in epoxy resin. Ultrathin sections (60-80 nm thick) were cut and stained with 2% uranyl acetate in 70% methanol and Reynolds lead citrate and observed using a transmission electron microscope operating at 80 kV (HT-7700; Hitachi, Tokyo, Japan).

## Genotoxicity test of new additives

Tests were performed for KP-457, TA-316, GNF-351, and Y-39983. The Ames test and chromosomal abnormality test were performed for all 4 drugs. Two drugs that were not negative in the chromosomal abnormality test were further subjected to micronucleus and Comet tests.

## In vivo general toxicity tests of iPSC-PLTs

A single-dose toxicity test of iPSC-PLTs was conducted using NOG mice (NOD/Shi-scid, IL-2R $\gamma$ KO Jic, SPF). Ten male and

10 female mice per group were injected IV with a suspension of  $2 \times 10^8$  platelets in a 0.1 mL volume or formulation buffer of the same volume. The mice were observed for their general condition, weight, and feeding amount, and underwent blood tests. On days 14 and 28, half of the mice in each group were sacrificed for autopsy and macroscopic observation of organs, organ weight, and histopathology.

Single and repeated (intermittent) administration tests were conducted using Crl:CD(SD) rats. Five male and 5 female rats per group were injected IV with a suspension of 40 mL/kg ( $\sim 16 \times 10^9$  platelets) from batch 13 or 20 mL/kg ( $\sim 8 \times 10^9$  platelets) from batch 14 for the single and repeated tests, respectively. Formulation buffer and saline of the same volume were used as controls. For repeated tests, samples were administered twice a week for a total of 4 times. Rats were observed for general condition, weight, and feeding amount, and underwent blood, urine, and ophthalmological tests for 2 weeks after the last dose. Finally, they were sacrificed for autopsy and macroscopic observation of organs, organ weight, and histopathology.

## In vitro tumorigenicity test

To assess imMKCLs, M35-1 imMKCL cells were irradiated with 25 Gy using the irradiation device of the blood transfusion cell therapy department used in the iPLAT1 study. The cells were then collected and resuspended in Dox-ON medium and cultured on MethoCult culture plates with  $1 \times 10^7$  imMKCLs with or without 100 nonirradiated imMKCLs per dish for 21 days, and the number of colonies that appeared was counted. Similarly,  $6.5 \times 10^6$  irradiated T1 iPSCs with or without  $6.5 \times 10^5$  nonirradiated T1 iPSCs were cultured for 18 days, and  $1 \times 10^7$  irradiated T1 HL60 cells with or without 100 nonirradiated T1 HL60 cells were cultured for 15 days.

To assess iPSC-PLTs in suspension culture, 2 mL of iPSC-PLTs irradiated with 25 Gy were cultured on MethoCult culture plates with or without 100 nonirradiated imMKCL cells for 22 days and 1000 nonirradiated HL60 cells per plate for 16 days, and the number of colonies that appeared was counted. Plates with imMKCL cells only and HL60 cells only were also prepared as control conditions. Similarly, for the adherent condition, 2 mL of iPSC-PLTs with or without 1000 nonirradiated HeLa cells or only HeLa cells were cultured for 12 days in minimum essential medium (Nacalai Tesque, #21443-15) with 15% fetal bovine serum and penicillin-streptomycin-glutamine.

## Hemostatic and circulation tests with rabbits

Experiments were performed based on recent reports.<sup>14,17</sup> Thrombocytopenia was induced by the subcutaneous administration of busulfan at 2 time points (18.75 mg/kg on day 0 and 22.5 mg/mL on day 3) in rabbits. On days 14 to 16, blood platelet counts of the busulfan-treated rabbits decreased to  $<2.5 \times 10^4/\mu$ L. To block the reticuloendothelial system and inhibit the rapid clearance of infused platelets due to xenografting, 0.75 mg/kg of emulsified ethylpalmitate was administered into the marginal ear vein 1 day before the platelet infusion. Subsequently,  $1 \times 10^{10}$  platelets per 2.5 kg body weight were injected into the left ear marginal vein at 1 mL per minute using a syringe pump under anesthesia. In the circulation model, splenectomy was performed 2 weeks before, and ethylpalmitate was administered 1 day before



platelet infusion. Blood sampling was performed from the ear marginal vein at 10 minutes; 20 minutes; and 1, 2.5, 4, 5.5, 7, and 24 hours after infusion. In the hemostasis model, bleeding times were measured at 2 sites of the right ear marginal vein wounded using a Quikheel Lancet (depth 1 mm, width 2.5 mm). In this hemostatic model, bleeding times of more than 600 seconds were defined as nonhemostatic.

### In vivo circulation in mice with IVIS

pcDNA3\_Venus-Akaluc was provided by RIKEN BRC through the National BioResource Project of the MEXT/AMED, Japan and subcloned using CS-CDF-UbCG- IRES GFP PRE (RIKEN BRC). A Venus-Akaluc-expressing imMKCL (Akaluc imMKCL) was established from M35-1 imMKCL using lentiviruses. Thrombocytopenia was induced by irradiating 2.4 Gy  $\gamma$  radiations to 10-week-old male NOG mice. Nine days after irradiation, the mice were infused with 100  $\mu$ L phosphate-buffered saline suspended with or without  $3 \times 10^6$  Akaluc imMKCL cells or  $2 \times 10^8$  Akaluc iPSC-PLTs into the tail vein under anesthesia (5 mice in each group). Venus-Akaluc was detected using an IVIS Lumina III (PerkinElmer) at 2, 6, 48, and 168 hours after administration.

## Results

### Establishment of imMKCL MCB

The imMKCL MCB was established from patient iPSCs (Figure 1). Patient iPSCs were generated from peripheral blood mononuclear cells (PBMCs) using episomal vectors, and 13 cryopreserved clones were verified for their ability to differentiate into megakaryocytes. Four clones capable of producing platelets were selected and confirmed to be negative for hepatitis C virus, hepatitis B virus, HIV, human T-lymphotropic virus type 1, and human parvovirus by quantitative PCR tests (qPCR). An iPSC clone T1 was differentiated to hematopoietic progenitor cells using the revised "PSC-sac" method.<sup>18,19</sup> Then, under the megakaryocyte differentiating condition, *c-MYC*, *BMI-1*, and *BCL-XL* were transduced by lentiviral vectors (supplemental Figure 1) to establish imMKCLs by conferring proliferation, antisenescence, and antiapoptosis capacity, respectively.<sup>11</sup>

After multiple attempts, 5 competent imMKCL clones were obtained in run M35, in which the initial differentiation into megakaryocytes was performed in 6 conditions: 3 multiplicity of infection conditions with and without the addition of SR1 (supplemental Table 1). After the second lentiviral infection, with which *BCL-XL* was transduced, we expanded 5 clones (M35-1, M35-2, M35-3, M35-5, and M35-6), and M35-1 was selected based on expandability and platelet production and subsequently stocked as the SCB in liquid nitrogen (supplemental Figure 2). The SCB imMKCL was then expanded and cryopreserved as an MCB, with which the virus and other safety tests were performed later.

Cells used in establishing the MCB were confirmed for sterility and potential pathogens, and the MCB was extensively tested for sterility and potential pathogens based on the materials used in the process (Table 1 and supplemental Tables 2-4). These results confirmed the compatibility of MCB for GMP production in terms of the negativity of possible pathogens. In addition, short tandem repeat analysis confirmed that the MCB was identical to the original iPSC clone and patient PBMCs (supplemental Table 5).

### Production of iPSC-PLTs using VerMES

The clinical trial product, "Autologous iPSC-PLTs," was produced from the M35-1 MCB under GMP-based conditions (Figure 2). The MCB vial was thawed and cultured with a thrombopoietin mimetic (TA-316),<sup>12</sup> stem cell factor, and doxycycline. In the next 23 days, the imMKCL was expanded more than 10 000 fold to  $2$  to  $4 \times 10^{10}$  in 20 L in 6 steps using increasing size culture plates, rotating flasks, and WAVE bags.

After the expansion culture, the cells were transferred to a medium without doxycycline but with a Rho-associated kinase inhibitor (Y-39983) and an arylhydrocarbon receptor antagonist (GNF-316), which together enable the feeder cell-free maturation of imMKCLs,<sup>14</sup> and with an ADAM17 inhibitor (KP-457), which prevents the shedding of GPIIb $\alpha$  (CD42b), a molecule indispensable for platelet adhesion and subsequent aggregation in vivo.<sup>13</sup> After 6-day maturation culture in 4 vessels of 8 L-scale VerMES bioreactors (supplemental Movie 1), iPSC-PLTs were purified, washed, and concentrated to the final package, including  $\sim 1.0 \times 10^{11}$  iPSC-PLTs in 200 mL bicarbonate Ringer's solution<sup>20</sup> with 10% ACD-A and 2.5% human serum albumin. The iPSC-PLTs were then  $\gamma$ -ray irradiated at a dose of 25 Gy to eliminate tumorigenicity. For the test batches, iPSC-PLTs were produced in small-scale flasks without being transferred to the WAVE and VerMES bioreactors.

### Characteristics and in vitro function of iPSC-PLTs

ABO type blood test results were negative for antigens A and B, although the patient had an A<sup>+</sup> blood type (Figure 3A). The surface expression in iPSC-PLTs was higher for CD41a, CD42b, CD61, and HLA-A/B/C but similar for CD36 and CD49b in primary platelets (Figure 3B). The HPA genotype of the MCB, including HPA-1b/b, matched the patient PBMCs (Figure 3C), and iPSC-PLTs were confirmed to be negative for HPA-1a antigen by flow cytometry analysis and the modified rapid monoclonal antibody-specific immobilization of platelet antigens (MR-MAIPA) assay (Figure 3D-F). The iPSC-PLTs were  $\sim 3.5$  to  $4 \mu$ m in diameter on average, which is larger than that of JRC-PLTs, which were  $\sim 2.5 \mu$ m in diameter (Figure 3G left). In accordance, because IPF is partly defined by forward light scatter, which reflects size, iPSC-PLTs showed a higher percentage of IPF (Figure 3G right). Nevertheless, the ultrastructures of iPSC-PLTs and JRC-PLTs were similar (Figure 3H).

Flow cytometric assays showed a competent response of iPSC-PLTs regarding P-selectin expression and PAC-1 binding, the common readout for in vitro platelet function, against ADP and TRAP-6 stimulation (Figure 4A-B). The aggregation assay also showed a competent response against ADP and collagen (Figure 4C). Various analysis results, such as the surviving platelet count and other flow cytometric analysis parameters, showed iPSC-PLTs within 5 days to have good quality and function (Figure 4D).

### Circulation and hemostasis in in vivo models

For the in vivo functional assessment of iPSC-PLTs, we adopted rabbit circulation and hemostasis models, in which JRC-PLTs were used to validate the system, and iPSC-PLTs produced from laboratory imMKCL clone CI-7 showed comparable functionality.<sup>14,17</sup> Based on these data, the model was approved as appropriate by

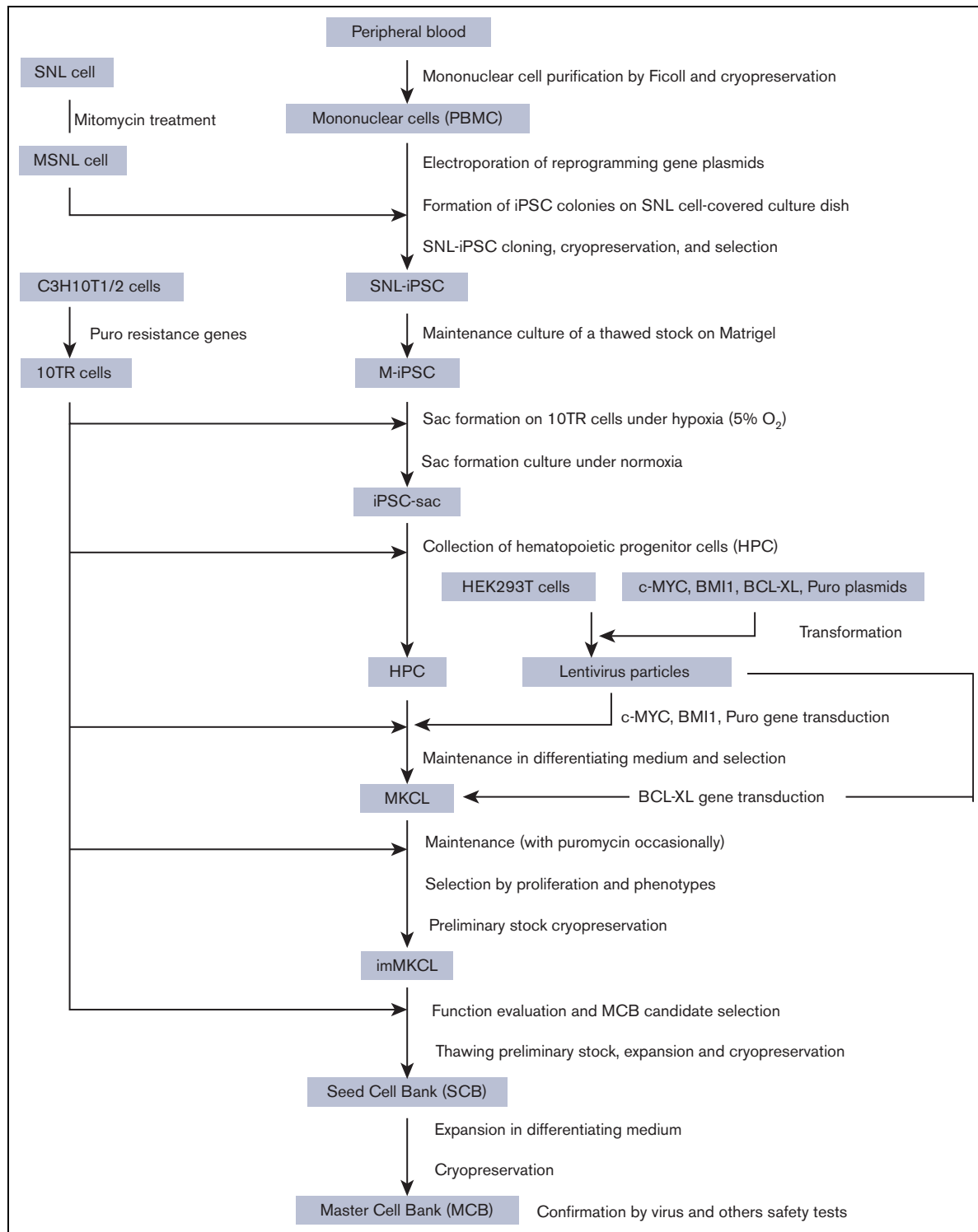


**Figure 1. Flowchart of MCB establishment from the patient's peripheral blood.** From the patient's peripheral blood, mononuclear cells were purified and subjected to reprogramming to iPSCs using SNL cells as feeder cells (SNL-iPSC) and then transferred on Matrigel (M-iPSC). Using the revised "PSC-sac" method, M-iPSCs were differentiated into hematopoietic progenitor cells. Then, under megakaryocyte differentiating condition, *c-MYC*, *BMI-1*, and *BCL-XL* were sequentially transduced by lentiviral vectors to establish imMKCLs. A single imMKCL clone was selected based on expandability and platelet production and stocked as seed cell banks (SCB) and then as an MCB in liquid nitrogen.

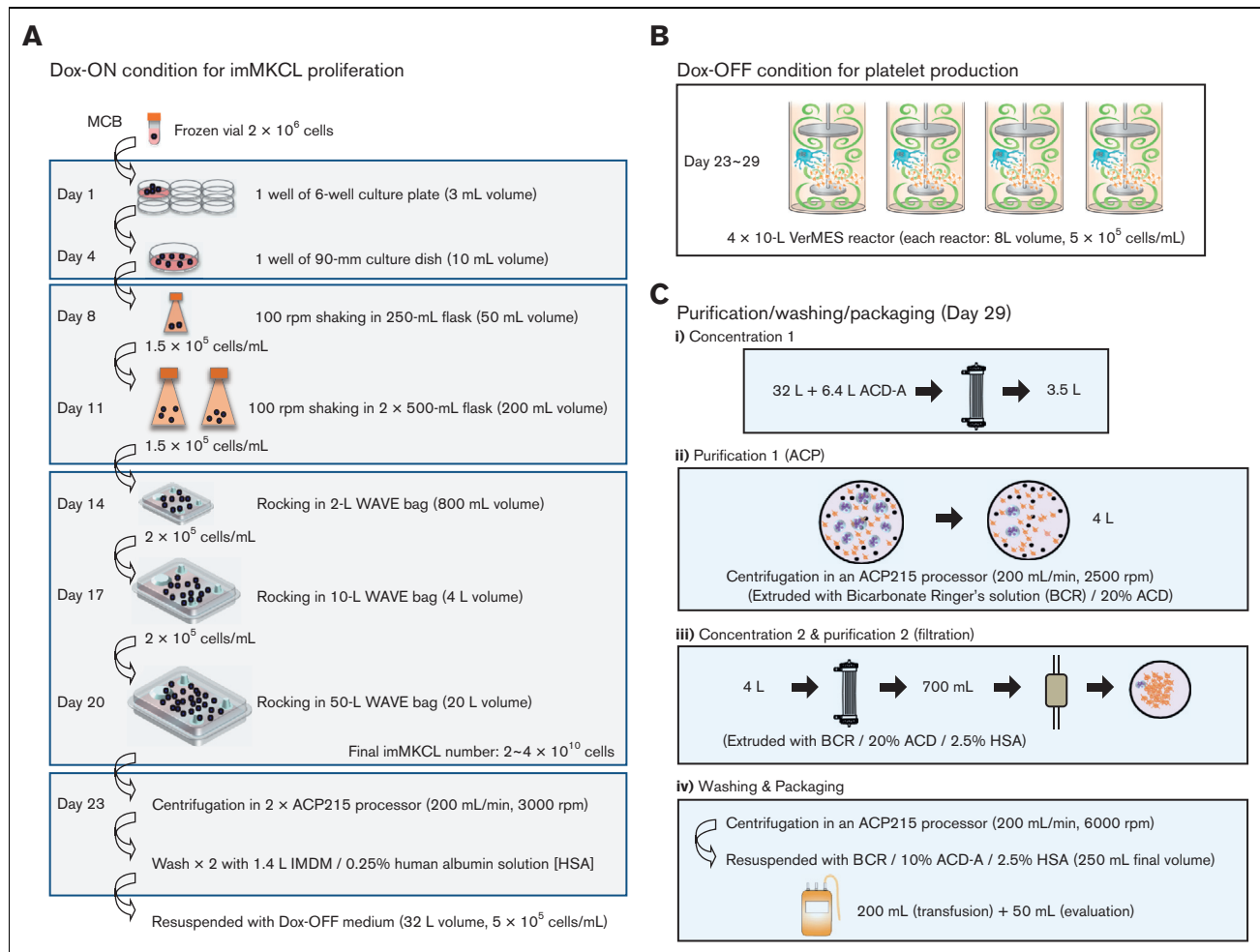


**Figure 2. Production process of iPSC-PLTs from the imMKCL MCB.** (A) Dox-ON condition for imMKCL proliferation: On day 1, the MCB cryopreserved in vials was thawed and cultured in a 6-well culture plate at  $37^\circ\text{C}$  and 5%  $\text{CO}_2$ . On days 4, 8, 11, 14, 17, and 20, the cells were transferred and cultured in a 90-mm culture dish, 250-mL culture flask, 2 500-mL culture flasks (both with 100 revolutions per minute [rpm] shaking), or 2-L, 10-L, and 50-L WAVE bags (each with rocking motion). On day 23, the imMKCLs were pelleted and washed twice using 2 ACP215 centrifugation systems and resuspended in Dox-OFF medium. (B) Dox-OFF condition for platelet production: the processed imMKCL solution was applied to 4 vessels of 10 L-scale VerMES bioreactors with 8 L medium solution in each and cultured with vertical stirring motion at  $37^\circ\text{C}$  for 6 days. (C) On day 29, the culture solution was added with 1/5 volume of ACD-A solution and concentrated to about 1/10 volume using a hollow fiber membrane filter. (Cii) imMKCLs and iPSC-PLTs were separated by continuous centrifugation using an ACP215 at 2500 rpm. With extruding solution, the platelet supernatant fraction volume became 4 L. (Ciii) The iPSC-PLT suspension was concentrated and extruded out to 700 mL using a hollow fiber membrane filter and then filtered through a leukocyte removal filter to remove residual megakaryocytes. (Civ) The iPSC-PLT suspension filtrate was centrifugated in an ACP215 at 200 mL per minute and 6000 rpm. Then, the pellets in the centrifuge pod were resuspended in 250 mL bicarbonate Ringer's solution (BRS) with 10% anticoagulant citrate dextrose solution (ACD)-A and 2.5% human serum albumin (HSA). From the 250 mL solution, 50 mL was drawn for evaluation.

Pharmaceuticals and Medical Devices Agency (PMDA), which is a Japanese regulatory agency. Using this rabbit model, the circulation of the patient's iPSC-PLTs initially dropped but thereafter stabilized from 2 to 7 hours (Figure 5A). Although no hemostasis was observed before transfusion of the patient iPSC-PLTs, 4 out of 4 lesions showed hemostasis within the set limit of 600 seconds (Figure 5B). To gain further insight into circulation after the iPSC-PLT clinical trial, we also performed IVIS imaging studies using patient imMKCLs introduced with Venus-Akaluc fluorescence-expressing vectors. Venus-Akaluc-expressing imMKCLs were observed seemingly trapped in the lungs. By contrast, Venus-Akaluc-expressing patient iPSC-PLTs showed systemic circulation and

preferential distribution compatible with the lung, liver, and spleen (Figure 5C-D), an observation similar to the patterns reported with general platelet transfusions in radiolabeling studies.<sup>21</sup>

### Safety profiles of iPSC-PLTs

The safety of iPSC-PLTs was extensively assessed through pre-clinical tests, the content of which was determined through consultation with the PMDA. The biological raw material standards set by the PMDA were applied to assure the pathogen-free state of the imMKCL MCB (Table 1 and supplemental Table 2-4) and the materials used for the GMP-grade production process starting from the MCB (see supplemental materials).

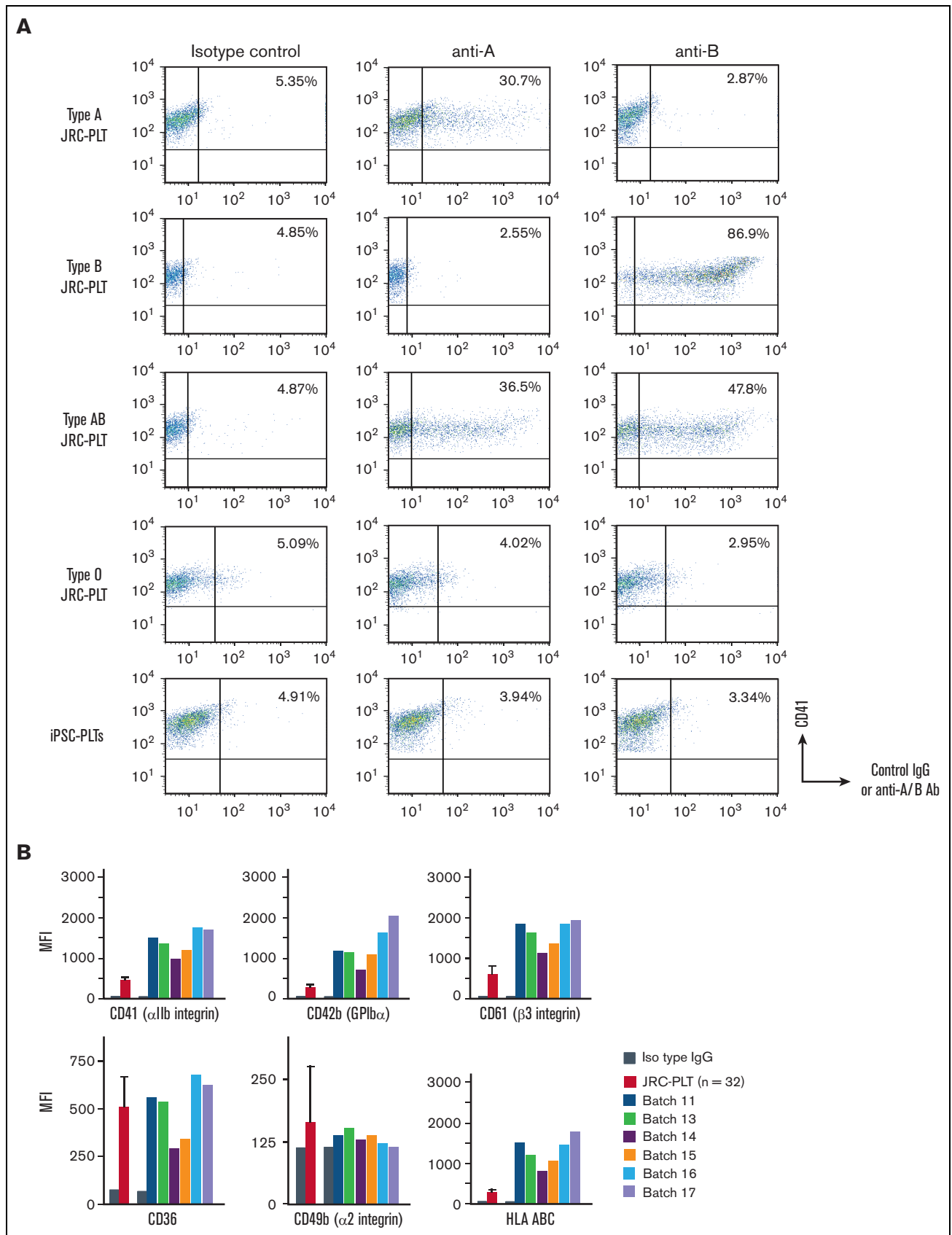
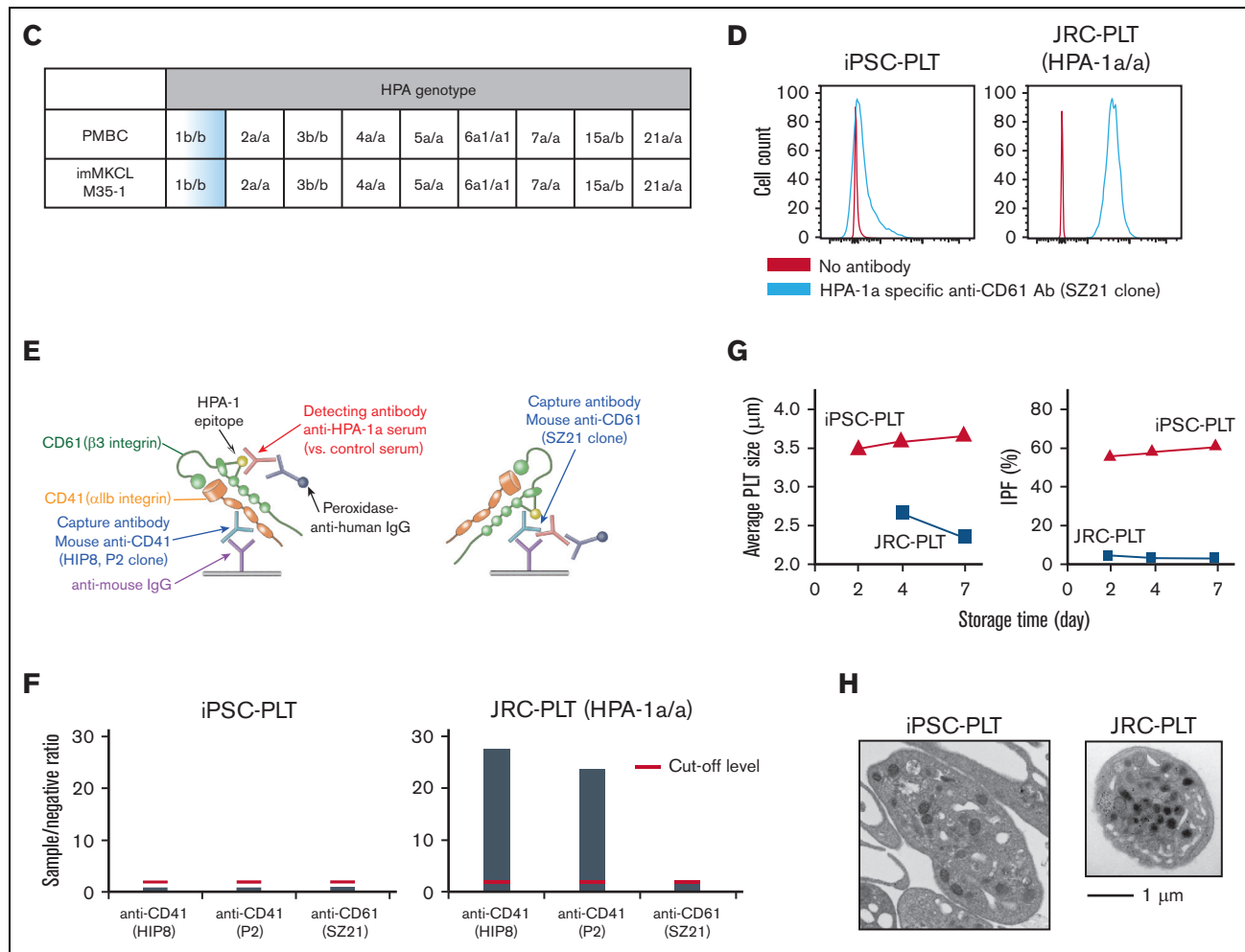


Figure 3.





**Figure 3 (continued). In vitro characteristics of iPSC-PLTs.** (A) Representative flow cytometry scatter plots of cell surface A antigen and B antigen expression on JRC-PLTs of types A, B, AB, and O and on iPSC-PLTs. (B) Flow cytometry analysis of JRC-PLTs and iPSC-PLTs of batch 11, 13, 14, 15, 16, and 17. Mean fluorescence intensities (MFI) of CD41, CD42b, CD61, CD36, CD49b, and HLA-A/B/C are shown. For JRC-PLTs, the mean and standard deviation of MFI from 32 individuals are shown. (C) HPA genotypes of patient PBMCs and M35-1 imMKCL, determined using WAKFlow HPA typing reagents. (D) Flow cytometry histogram of iPSC-PLTs and HPA-1a/1a JRC-PLTs using HPA-1a-specific anti-CD61 (clone SZ21) antibody. (E) Scheme of the MR-MAIPA assay to identify HPA-1a antigen expression. (F) Readout ratio of anti-HPA-1a serum to negative control serum for iPSC-PLTs and HPA-1a/1a JRC-PLTs by MR-MAIPA, as in panel C. SZ21 antibody blocks the binding of anti-HPA-1a serum, resulting in values below the cutoff level for JRC-PLTs as well, thereby assuring specificity of the serum. (G) Sizes and percentages of the large IPF corresponding to iPSC-PLTs (batch 18) and blood donor-derived JRC-PLTs at different storage days. Representative data of 3 batches are shown. (H) Representative transmission electron micrograph images of iPSC-PLTs (batch 17) and JRC-PLTs. Scale bar: 1 μm.

Using test batches, the nonclinical safety evaluation of the iPSC-PLTs was performed. Residual concentrations of novel drugs in the final product were below the limit based on the International Council for Harmonisation of Technical Requirements for Registration of Pharmaceuticals for human use M7 guideline, and genetic toxicity tests confirmed no mutagenesis potential (Figure 6A). Single-dose testing in NOG mice and single and repeated-dose testing in rats confirmed no toxicity of iPSC-PLTs (Figure 6B and C).

Karyotype analysis revealed abnormalities in iPSCs after 20 passages and in the MCB (supplemental Table 6), raising concerns regarding genomic instability and tumorigenicity. However, the tumorigenic

potential was considered negative based on in vitro tumorigenicity tests, which showed no proliferating cell colonies for both imMKCLs and iPSC-PLTs after irradiation at 25 Gy (Figure 6D).

## Discussion

In this study, we established a GMP-based system using imMKCLs as an MCB with turbulent flow-based bioreactors and 4 novel agents for the production of clinically required  $10^{11}$ -scale iPSC-PLTs.<sup>11,14</sup> We also performed an extensive nonclinical evaluation of MCB and iPSC-PLTs to confirm their quality, efficacy, and safety. Other researchers have also developed iPSC-derived

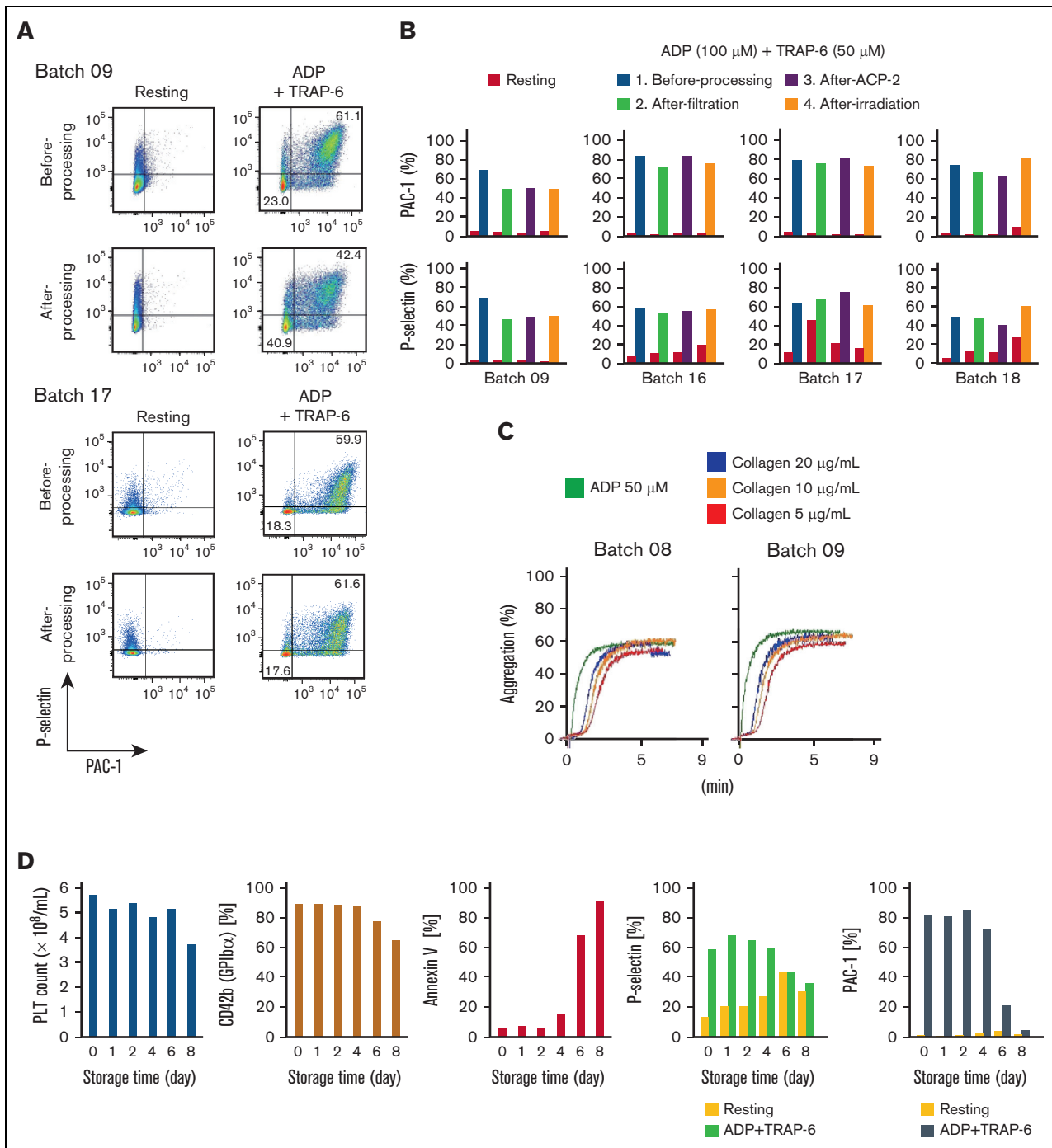


**Figure 4. In vitro functional assessment of iPSC-PLTs shows the comparability with blood donor-derived platelets.** (A) Representative flow cytometry images of P-selectin expression and PAC-1 binding of iPSC-PLTs (batch 09 and 17) with or without 100  $\mu\text{M}$  ADP and 40  $\mu\text{M}$  TRAP-6. (B) Flow cytometry data as in panel A for 4 batches of iPSC-PLT samples before processing, after filtration, and after the second ACP215 centrifugation for washing and after irradiation. (C) Aggregation assay. iPSC-PLTs (batch 07 and 09) were stimulated with 50  $\mu\text{M}$  ADP or 5, 10, and 20  $\mu\text{g}/\text{mL}$  collagen. (D) Autologous iPSC-PLTs of batch 16 in a blood bag were stored in a platelet preservation shaker. At the manufacturing date and after storage for 1, 2, 4, 6, and 8 days, the samples were tested for platelet count, CD42b expression, annexin V binding and in vitro function, and PAC-1 binding and P-selectin expression with or without ADP + TRAP-6 stimulation.

Downloaded from [http://ashpublications.org/bloodadvances/article-pdf/6/23/6056/20187981blooda\\_adv-2022-008512-main.pdf](http://ashpublications.org/bloodadvances/article-pdf/6/23/6056/20187981blooda_adv-2022-008512-main.pdf) by guest on 14 December 2022

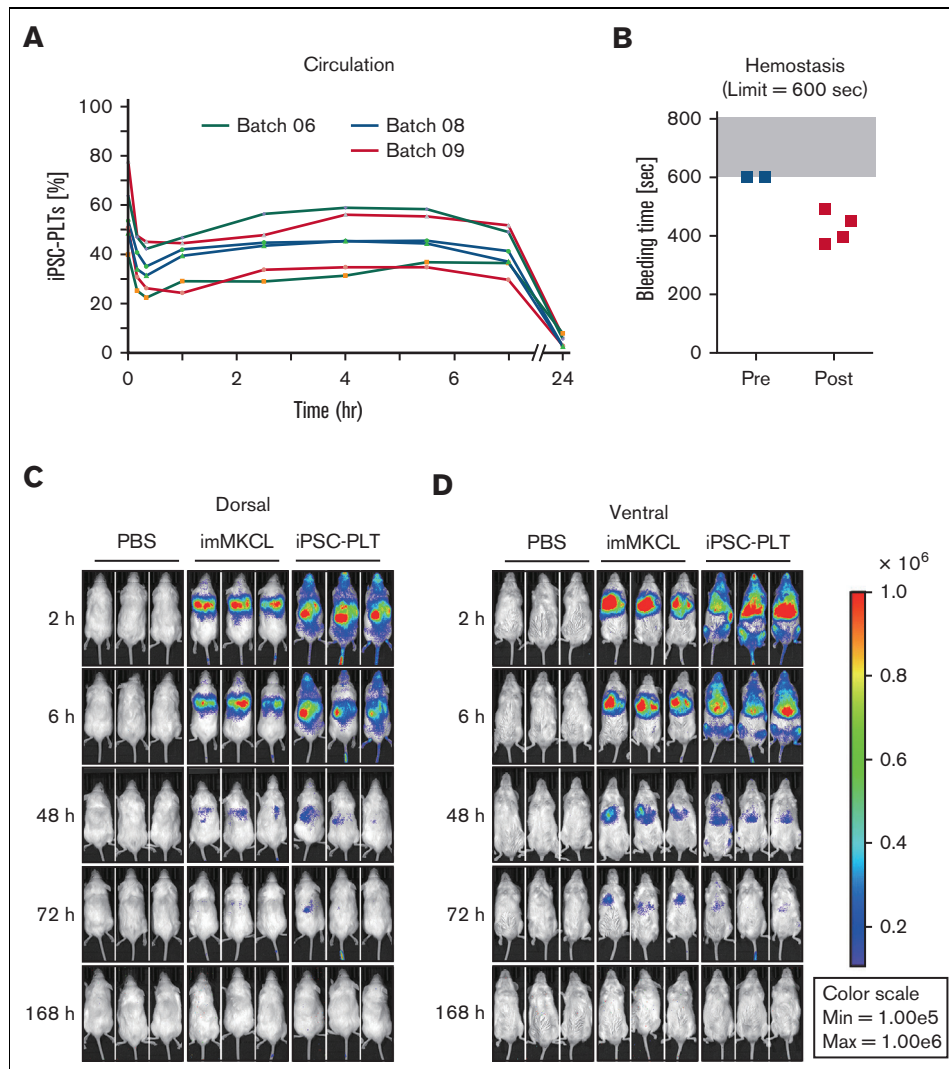


**Figure 5. In vivo functional assessment of iPSC-PLTs.** (A) In vivo circulation in thrombocytopenic rabbit models for 3 batches of iPSC-PLTs as measured by the percentage of human and rabbit platelets in peripheral blood using flow cytometry. (B) In vivo hemostasis in thrombocytopenic rabbit models for iPSC-PLTs, as measured by the bleeding time of the ear incision before and after the transfusion of human iPSC-PLTs (batch 09). The maximum time was set to 600 seconds. (C) Circulation of iPSC-PLTs in NOG mice by IVIS imaging: imMKCLs or iPSC-PLTs expressing Venus-Akaluc were injected into NOG mice. Phosphate-buffered saline was injected for the control group. After 2, 6, 48, 72, and 168 hours, the mice were subjected to IVIS imaging.

expandable megakaryocytes<sup>22</sup> and bioreactors to yield platelets from megakaryocytes, but clinical scale production has not been reported.<sup>6,9,10</sup> Meanwhile, the same rule for using progenitor cells from the MCB rather than iPSCs could be applied to other cell types in regenerative medicine.

Establishing an imMKCL clone with competent proliferative and platelet-yielding capacities required extensive attempts in the current case. Based on the crucial level of c-MYC,<sup>23</sup> we prepared variance in the multiplicity of infection of a lentiviral vector that included c-MYC and also conditions with or without the addition of SR-1. However, 5 out of 6 conditions generated imMKCLs in run M35, suggesting that the loading range of c-MYC transduction and the addition of SR-1 were not the only key determinants. The difficulty may be due to epigenetic characteristics that stem from the original iPSC clone.<sup>24</sup> We also found that the silencing of CDKN1A and p53 can improve the stable establishment of

imMKCLs.<sup>25</sup> Further studies are ongoing to determine the properties of the original iPSC clone and the procedure to establish imMKCLs that determine the final imMKCL competency.

To produce autologous iPSC-PLTs from MCB, we set up a production system comprising a 23-day Dox-ON expansion phase, a 6-day Dox-OFF platelet production phase, and a final 1-day purification-washing-packaging phase. To achieve the production of  $10^{11}$ -scale competent iPSC-PLTs ex vivo, an efficient and scalable bioreactor was required. A turbulent flow-based VerMES bioreactor, with the identification of 2 determinant parameters, shear stress, and turbulent energy, was found to be suitable. However, the production of platelets is  $\sim 100$  per cell from imMKCLs, still significantly less than the estimated 800 to 2000 per cell from megakaryocytes in vivo.<sup>26</sup> This difference may reflect the nature of iPSC-derived megakaryocytes being mostly embryonic or fetal type, which expands more but yields fewer platelets compared with adult

**Table 1. Virus and other safety tests of the M35-1 imMKCL MCB**

Item	Method	Criterion	Result
1. Sterility test (bacteria and fungus)	Direct culture (JP, USP, and EP compatible)	Negative	Negative
2. Mycoplasma test	Agar and nonagar culture (JP, USP, and EP compatible)	Negative	Negative
3. Virus tests			
General in vitro test	28-day cell culture (Vero, MRC, BHK, HeLa, and NIH3T3)	Negative	Negative
General in vivo test	Mouse and infant mouse, embryonated egg administration	Negative	Negative
Detection test			
Mouse virus	Mouse antibody production	Negative	Negative
Rat virus	Rat antibody production	Negative	Negative
Hamster virus	Hamster antibody production	Negative	Negative
Human virus	qPCR of 14 virus (HIV-1/2, human T-lymphotropic virus type 1/2, hepatitis A virus, hepatitis B virus, hepatitis C virus, HHV-6, HHV-7, HHV-8, cytomegalovirus, Epstein-Barr virus, simian virus 40, and parvovirus B19)	Negative	Negative
Bovine/swine virus	FDA 9 CRF method	Negative	Negative
Circovirus	qPCR	Negative	Negative
Bovine Parvovirus	qPCR	Negative	Negative
Swine hepatitis E virus	qPCR	Negative	Negative
Torque Teno virus	qPCR	Negative	Negative
Mouse endogenous virus			
Reverse transcriptase	F-PERT high sensitivity reverse transcriptase activity detection	Negative	Negative
Electron microscope (transmission electron microscope)	Observation of 200 cells	Negative	Negative
S + L-focus assay			
Replication competent retrovirus	Xenogenic retrovirus detection	Negative	Negative
Aves virus	Detection of replication competent retrovirus in the cell qPCR (adenovirus, chicken parvovirus, avian encephalomyelitis, canine adenovirus, and Reovirus)	Negative	Negative
Equine virus		Negative	Negative
Insect virus	FDA 9 CFR method qPCR (Flock house virus, Nodamura virus, Booralla virus, and Pariacoto virus)	Negative	Negative
4. In vitro tumorigenicity	Colony forming after $\gamma$ -ray irradiation	Compatible	Compatible

JP, Japanese Pharmacopeia; USP, Unites States Pharmacopeia; EP, European Pharmacopeia; CFR, Code of Federal Regulations; FDA, Food and Drug Administration; HHV, human herpesvirus; F-PERT, fluorescent-product enhanced reverse transcriptase.

megakaryocytes. Meanwhile, the purification-washing-packaging stage resulted in a 50% loss of iPSC-PLTs. Improvements in this step could result in a higher yield by developing, for instance, a filtering system optimized for this purpose.

The higher expression of certain surface antigens may be due to the larger size of iPSC-PLTs compared with JRC-PLTs. Meanwhile, the expression of CD36 and CD49 was similar, indicating lower expression per surface area. While this difference, along with the negativity of A antigens, may be iPSC-PLT-specific with an unknown cause, no apparent difference in functionality in preclinical studies was observed.

The circulation in rabbits showed an initial dip followed by a moderate increase that plateaued for over 6 hours. This was observed in our previous study using laboratory strain-derived iPSC-PLTs.<sup>14</sup> Given that the size of circulating iPSC-PLTs decreases over time

after a transfusion and that there is a substantial accumulation in the lungs according to this IVIS study, the larger fraction of iPSC-PLTs had likely fragmented, resulting in the moderate increase.

Regarding tumorigenicity, anucleate platelets themselves are not of concern, but imMKCLs, which harbor a c-MYC transgene, and possibly iPSCs, which are known to form teratoma,<sup>4-8</sup> remain in the product. Moreover, karyotype analysis revealed abnormalities in the original iPSCs upon culture and in the imMKCL MCB. However, imMKCLs did not proliferate in the absence of doxycycline. Finally, radiation with 25 Gy, as is usually done for blood products, was performed to eliminate tumorigenicity. The applicability of radiation is an advantage in ensuring the safety of iPSC-PLTs over the infusion of megakaryocytes<sup>27</sup> or other nucleate cell-based grafts in regenerative medicine.

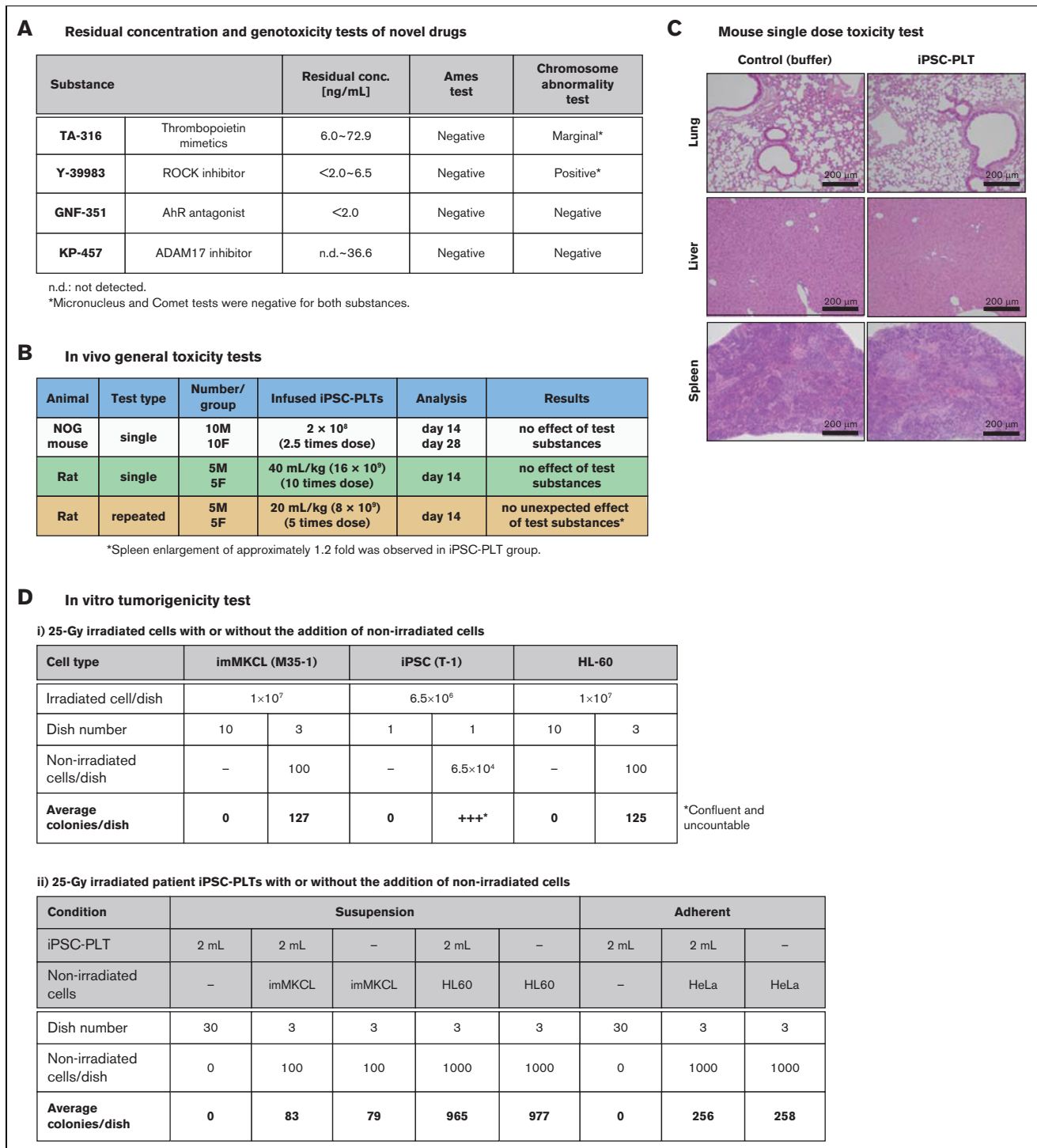


**Figure 6. Nonclinical safety assessment of iPSC-PLTs.** (A) Profiles of novel drugs in the test batches. All substances were a less-than-lifetime limit of 120 μg per day for administration of up to 1 month. (B) A table summarizing in vivo general toxicity tests. For the single-dose study in NOG mice, the mice were observed for general condition, weight, and feeding amount, and underwent blood tests. On days 14 and 28, half of the mice in each group were sacrificed for autopsy for macroscopic observation of the organs, organ weight, and histopathology. For single and repeated administration tests on rats, the rats were observed for general condition, weight, and feeding amount and underwent blood, urine, and ophthalmological tests for 2 weeks after the last dose. They were then sacrificed for autopsy for macroscopic observation of the organs, organ weight, and histopathology. Formulation buffer and saline of the same volume were used as controls. For repeated tests, samples were administered twice a week 4 times. (C) Hematoxylin and eosin-stained histology sections of day 14 NOG mice injected IV with a 0.1 mL suspension of 2 × 10<sup>8</sup> platelets or formulation buffer of the same volume. (D) In vitro tumorigenicity test. (i) imMKCLs, iPSCs, or HL60 cells were cultured with or without the same nonirradiated cell type in 90-mm culture dishes. The number of grown colonies per dish was counted and averaged. (ii) An iPSC-PLT product of 2 mL and nonirradiated imMKCLs or HL60 cells were cultured in different combinations in suspension culture condition in 90-mm culture dishes. Similarly, an iPSC-PLT product of 2 mL and nonirradiated HeLa cells were cultured in different combinations in adherent culture condition in 90-mm culture dishes. The number of grown colonies per dish was counted and averaged.



In conclusion, to provide a compatible platelet product for patient with allo-PTR with no compatible platelet donors, we established a production system of autologous iPSC-PLTs and performed extensive nonclinical evaluation. The GMP-based production and nonclinical tests were decided through consultation with the PMDA. The autologous iPSC-PLTs were thus determined to be compatible with the iPLAT1 clinical trial. Beyond the trial, this study will lead to the development of allogeneic iPSC-PLTs for low cost off-the-shelf use. It will also serve as a complete resource for the development of other stem cell-derived platelet products and could be referred to any stem cell-derived cells that use progenitor cells instead of iPSCs as the MCB.

## Acknowledgments

The authors would like to thank the staff at the CiRA Foundation and members of the Eto lab (CiRA, Kyoto University) for the iPSC-PLT production, evaluation, and technical assistance; Peter Karagiannis (CiRA) for proofreading this article; the Japanese Red Cross Society for providing donor-derived human platelets and plasma; and Tadaaki Hanatani and Yuji Arakawa (CiRA) for helpful comments and support. This work was financially supported by grants from the Japan Agency for Medical Research and Development: The Highway Program for Realization of Regenerative Medicine (JP17bm0504008; Eto) and Core Center for iPS Cell Research (JP17bm0104001; Sugimoto, Nakamura, Eto), and a grant-in-aid for scientific research (S) (21H05047) (K.E.) from the Japan Society for the Promotion of Science.

## Authorship

Contribution: N.S. designed and performed the research, analyzed the data, and wrote the paper; S.N., S.S., and A. Shigemasa designed and performed the experiments, produced the

product, and analyzed the data; J.K., D.M., and K-RK provided samples and designed the study. N.M., M.T., T.H., and A.F. designed and performed the experiments and analyzed the data; M.N. and N.W. designed and performed the experiments and analyzed the data; M.H., Y.T., and S.O. supervised experiments; A. Sawaguchi designed and performed the experiments and analyzed the data; A.T-K. supervised the studies; and K.E. designed and supervised the research and wrote the manuscript.

Conflict-of-interest disclosure: S.N. and K.E. have applied for patents related to this manuscript. N.S. serves as a consultant for Megakaryon Co. J.K. serves as a consultant for Astellas Pharma and an adviser for Daiichi Sankyo Co, Janssen Pharmaceutical, Megakaryon, SymBio Pharmaceuticals, and Takeda Pharmaceutical and receives research funding from Eisai Co. A. Shigemasa is employed at Megakaryon. A.T-K. serves as an adviser for Megakaryon and receives research funding from Ono Pharmaceutical. K.E. is a founder of Megakaryon and a member of its scientific advisory board without salary and receives research funding from Megakaryon, Otsuka Pharmaceutical, and Kyoto Manufacturing Co. The remaining authors declare no competing financial interests. All the interests were reviewed and are managed by Kyoto University in accordance with its conflict-of-interest policies.

ORCID profiles: N.S., [0000-0002-7271-9175](https://orcid.org/0000-0002-7271-9175); S.N., [0000-0002-5601-9777](https://orcid.org/0000-0002-5601-9777); J.K., [0000-0002-6704-3633](https://orcid.org/0000-0002-6704-3633); M.T., [0000-0002-9024-6818](https://orcid.org/0000-0002-9024-6818); T.H., [0000-0002-1776-0052](https://orcid.org/0000-0002-1776-0052); A.F., [0000-0003-3387-1817](https://orcid.org/0000-0003-3387-1817); M.N., [0000-0002-4835-2545](https://orcid.org/0000-0002-4835-2545); S.O., [0000-0002-6257-4152](https://orcid.org/0000-0002-6257-4152); A.T-K., [0000-0001-7678-4284](https://orcid.org/0000-0001-7678-4284); K.E., [0000-0002-5863-7122](https://orcid.org/0000-0002-5863-7122).

Correspondence: Koji Eto, Department of Clinical Application, CiRA, Kyoto University, 53 Kawaharacho, Shogoin, Sakyo, Kyoto 606-8507, Japan; email: [kojiето@cira.kyoto-u.ac.jp](mailto:kojiето@cira.kyoto-u.ac.jp).

## References

1. Szczepiorkowski ZM, Dunbar NM. Transfusion guidelines: when to transfuse. *Hematol Am Soc Hematol Educ Prog*. 2013;2013:638-644.
2. Estcourt LJ, Birchall J, Allard S, et al. Guidelines for the use of platelet transfusions. *Br J Haematol*. 2017;176(3):365-394.
3. Stanworth SJ, Navarrete C, Estcourt L, Marsh J. Platelet refractoriness—practical approaches and ongoing dilemmas in patient management. *Br J Haematol*. 2015;171(3):297-305.
4. Takahashi K, Yamanaka S. Induction of pluripotent stem cells from mouse embryonic and adult fibroblast cultures by defined factors. *Cell*. 2006;126(4):663-676.
5. Takahashi K, Tanabe K, Ohnuki M, et al. Induction of pluripotent stem cells from adult human fibroblasts by defined factors. *Cell*. 2007;131(5):861-872.
6. Blau HM, Daley GQ. Stem cells in the treatment of disease. *N Engl J Med*. 2019;380(18):1748-1760.
7. Yu J, Vodyanik MA, Smuga-Otto K, et al. Induced pluripotent stem cell lines derived from human somatic cells. *Science (New York, NY)*. 2007;318(5858):1917-1920.
8. Park IH, Zhao R, West JA, et al. Reprogramming of human somatic cells to pluripotency with defined factors. *Nature*. 2008;451(7175):141-146.
9. Sim X, Poncz M, Gadue P, French DL. Understanding platelet generation from megakaryocytes: implications for in vitro-derived platelets. *Blood*. 2016;127(10):1227-1233.
10. Sugimoto N, Eto K. Generation and manipulation of human iPSC-derived platelets. *Cell Mol Life Sci*. 2021;78(7):3385-3401.
11. Nakamura S, Takayama N, Hirata S, et al. Expandable megakaryocyte cell lines enable clinically applicable generation of platelets from human induced pluripotent stem cells. *Cell Stem Cell*. 2014;14(4):535-548.
12. Aihara A, Koike T, Abe N, et al. Novel TPO receptor agonist TA-316 contributes to platelet biogenesis from human iPS cells. *Blood Adv*. 2017;1(7):468-476.

13. Hirata S, Murata T, Suzuki D, et al. Selective inhibition of ADAM17 efficiently mediates glycoprotein Iba $\alpha$  retention during ex vivo generation of human induced pluripotent stem cell-derived platelets. *Stem Cells Transl Med.* 2017;6(3):720-730.
14. Ito Y, Nakamura S, Sugimoto N, et al. Turbulence activates platelet biogenesis to enable clinical scale ex vivo production. *Cell.* 2018;174(4):636-648.
15. Hayashi T, Aminaka R, Ishii H, et al. Frequency of allotype "b" in human platelet antigen 1 to 29 systems among blood donors in Japan estimated using high-resolution melt analysis. *Transfusion.* 2020;60(11):2702-2713.
16. Campbell K, Rishi K, Howkins G, et al. A modified rapid monoclonal antibody-specific immobilization of platelet antigen assay for the detection of human platelet antigen (HPA) antibodies: a multicentre evaluation. *Vox Sang.* 2007;93(4):289-297.
17. Watanabe N, Nogawa M, Ishiguro M, et al. Refined methods to evaluate the in vivo hemostatic function and viability of transfused human platelets in rabbit models. *Transfusion.* 2017;57(8):2035-2044.
18. Takayama N, Nishikii H, Usui J, et al. Generation of functional platelets from human embryonic stem cells in vitro via ES-sacs, VEGF-promoted structures that concentrate hematopoietic progenitors. *Blood.* 2008;111(11):5298-5306.
19. Yuzuriha A, Nakamura S, Sugimoto N, et al. Extracellular laminin regulates hematopoietic potential of pluripotent stem cells through integrin beta1-ILK-beta-catenin-JUN axis. *Stem Cell Res.* 2021;53:102287.
20. Oikawa S, Taguchi T, Endo K, et al. Storage of washed platelets in BRS-A platelet additive solutions based on two types of clinically available bicarbonated Ringer's solutions with different electrolyte concentrations. *Transfus Apher Sci.* 2015;53(2):233-237.
21. Peters AM. Review of platelet labelling and kinetics. *Nucl Med Commun.* 1988;9(10):803-808.
22. Moreau T, Evans AL, Vasquez L, et al. Large-scale production of megakaryocytes from human pluripotent stem cells by chemically defined forward programming. *Nat Commun.* 2016;7:11208.
23. Takayama N, Nishimura S, Nakamura S, et al. Transient activation of c-MYC expression is critical for efficient platelet generation from human induced pluripotent stem cells. *J Exp Med.* 2010;207(13):2817-2830.
24. Nishizawa M, Chonabayashi K, Nomura M, et al. Epigenetic variation between human induced pluripotent stem cell lines is an indicator of differentiation capacity. *Cell Stem Cell.* 2016;19(3):341-354.
25. Sone M, Nakamura S, Umeda S, et al. Silencing of p53 and CDKN1A establishes sustainable immortalized megakaryocyte progenitor cells from human iPSCs. *Stem Cell Rep.* 2021;16(12):2861-2870.
26. Lefrancais E, Ortiz-Munoz G, Cadrillier A, et al. The lung is a site of platelet biogenesis and a reservoir for haematopoietic progenitors. *Nature.* 2017; 544(7648):105-109.
27. Wang Y, Hayes V, Jarocha D, et al. Comparative analysis of human ex vivo-generated platelets vs megakaryocyte-generated platelets in mice: a cautionary tale. *Blood.* 2015;125(23):3627-3636.